CRISPR knockout of winter-biased *SUT4* alters phenology, biomass accrual, and fertility of field-grown hybrid poplar

Trevor T. Tuma[1], Holly A. McInnes[1,2], Hongduyen Pham[1,3], William P. Bewg[1,4], Michihito Deguchi[1,4], Ran Zhou[1,4], Samantha M. Surber[2], Anna Lipzen[5], Kerrie W. Barry[5], Brent Lieb[1], Daniela L. Weber Wyneken[1], Anne E. Harman-Ware[6], Joseph Dahlen[1], Scott A. Harding[1,4], and Chung-Jui Tsai[1,2,4]

[1] Warnell School of Forestry and Natural Resources, University of Georgia, Athens, GA, 30602, USA.

[2] Department of Plant Biology, University of Georgia, Athens, GA, 30602, USA.

[3] Department of Biochemistry & Molecular Biology, University of Georgia, Athens, GA, 30602, USA.

[4] Department of Genetics, University of Georgia, Athens, GA, 30602, USA.

[5] DOE Joint Genome Institute, Lawrence Berkeley National Laboratory, Berkeley, CA, 94720, USA

[6] National Bioenergy Center, National Renewable Energy Laboratory, Golden, CO 80401, USA.

Key words: SUT, poplar, winter, sterility, biomass, field trial

Running head: Field performance of *sut4* poplar

Corresponding author: Chung-Jui Tsai (cjtsai@uga.edu)

Abstract

Woody perennial trees annually transition between photoautotrophic and heterotrophic states. As carbohydrate accumulation and utilization patterns shift, so does the expression of genes encoding various sucrose-proton symporters (SUTs). The poplar genome contains five *SUT* gene family members involved in intracellular and long-distance sucrose transport. Among these, only the single-copy *SUT4* and the *SUT5/SUT6* genome duplicates are expressed year-round, with *SUT4* strongly expressed in winter. Using CRISPR mutagenesis, we investigated the role of winter-expressed *SUTs* in carbohydrate allocation, biomass accrual, seasonal phenology, and sexual reproduction in *Populus tremula* × *P. alba* under field conditions. In *sut4* mutants, fall leaf senescence occurred earlier and spring bud flush was delayed compared to controls, resulting in reduced diameter and overall height growth. These mutants also exhibited altered sugar partitioning and reduced levels of raffinose family oligosaccharides, which are typically associated with cold and desiccation tolerance. Knockouts of *SUT5* and *SUT6*, whether single or double, did not affect seasonal phenology or overall tree growth. All genotypes flowered precociously after two years in the field, but *sut4* catkins accumulated abnormally high levels of sucrose, galactinol, and raffinose. Transcriptome profiling showed down-regulation of genes associated with proanthocyanidin biosynthesis and vacuolar transport, and up-regulation of genes involved in protein oligomerization, misfolding, and refolding responses. Development of *sut4* ovules was compromised, and no seeds were produced in *sut4* catkins following controlled pollination. Our findings suggest that the single-copy tonoplast SUT4 may be more critical than other SUTs for mitigating stress associated with winter fitness and growth transitions during cool seasons.

Introduction

Woody trees annually cycle through periods of active growth, leaf senescence and abscission, dormant bud quiescence, and bud break in accordance with temperature and day length cues (Rohde and Bhalerao, 2007; Cooke et al., 2012; Savage and Chuine, 2021). The timing of such environmental cues influences plant phenology, which ultimately determines perennial biomass growth in temperate and boreal regions with freezing winter temperatures (Keunen et al., 2013; Kuster et al., 2014; Zohner et al., 2021). In sink organs that remain active after fall senescence, reserves of nonstructural carbohydrates (NSC) are utilized to sustain winter survival (Kozlowski, 1992). During the winter, NSC reserves are converted to sugar and oligosaccharide (e.g., galactinol, raffinose, stachyose) pools for basal metabolism, respiration, membrane stabilization, reactive oxygen species (ROS) scavenging, and protection against frost and freezing damage (Ameglio et al., 2004; Regier et al., 2010). With the arrival of spring, NSC reserves are remobilized to fuel the emergence of new organs, including flowers, leaves, and vasculature, before resumption of photosynthesis (Loescher et al., 1990; Tixier et al., 2019). Not surprisingly, seasonal variation in NSC dynamics is observed across various phylogenetic groups (e.g., gymnosperms, angiosperms), life habits (e.g., evergreen, deciduous), and climate biomes (e.g., boreal, temperate, Mediterranean, tropical) (Martínez-Vilalta et al., 2016; Palacio et al., 2018; Furze et al., 2019).

Although studied to a lesser extent, seasonal changes in the expression of genes involved in NSC synthesis, utilization, and transport have been reported (Ko et al., 2011; Dobbelstein et al., 2018; Jokipii-Lukkari et al., 2018). Genes associated with starch hydrolysis and the biosynthesis of

raffinose family oligosaccharides (RFOs) are most strongly expressed during winter dormancy when starch is depleted and RFOs accumulate in the stems of poplar (*Populus trichocarpa*) and Norway spruce (*Picea abies*) (Kozlowski, 1992; Schrader et al., 2004; Regier et al., 2010; Ko et al., 2011; Jokipii-Lukkari et al., 2018). Various carbohydrate transporters also exhibit seasonal expression patterns. In poplar, the vascular-specific Type I *SUT* (the *SUT1* and *SUT3* genome duplicates) transcripts are only detected in the summer, whereas the broadly expressed Type II (the *SUT5* and *SUT6* genome duplicates) and Type III (single-copy *SUT4*) transcripts are detected year-round, with *SUT4* being strongly winter-biased (Ko et al., 2011; Sreedasyam et al., 2023; Tuma et al., 2024). The divergent seasonal expression patterns observed amongst members of the *SUT* gene family have also been reported in Norway spruce (*Picea abies*), beech (*Fagus sylvatica*), and oak (*Quercus robur*) (Dobbelstein et al., 2018), hinting at season-specific roles in the utilization of NSC throughout the year.

The summer-biased expression of poplar *SUT1* and *SUT3* is consistent with the involvement of these Type I plasma membrane symporters in lateral sucrose partitioning during stem secondary growth (Mahboubi et al., 2013). The physiological function of the Type II plasma membrane SUTs remains unspecified in any species (Peng et al., 2014). The tissue distribution of poplar *SUT5* and *SUT6* transcripts is distinct from that of summer-biased plasma membrane isoforms, but more similar to that of the winter-biased tonoplast isoform (Payyavula et al., 2011). The poplar tonoplast SUT4 is the predominant SUT isoform in source leaves, modulating sucrose efflux from the vacuole and impacting the transport of sucrose from source to sink organs (Payyavula et al., 2011). The effects of *SUT4*-knockdown (KD) or knockout (KO) on plantwide sucrose homeostasis, starch utilization, turgor control, osmotic adjustment, and sensitivity to

94 drought and defoliation treatments have been reported (Payyavula et al., 2011; Xue et al., 2016;
95 Harding et al., 2020; Harding et al., 2022). Recently, we extended our investigation to uncover
96 an effect of SUT4 on the dynamics of NSC reserves in sink organs during heterotrophic growth.
97 Following stem coppicing, *SUT4*-KO poplars showed delayed epicormic bud emergence and
98 reduced biomass in winter but not summer glasshouse conditions (Tuma et al., 2024). The results
99 contrasted those of previous reports showing subtle growth differences between *SUT4*-KD and
100 wild type (WT) plants when grown under relatively stable and controlled glasshouse conditions
101 (Payyavula et al., 2011; Frost et al., 2012), suggesting that SUT4 plays a critical role in
102 supporting growth under cooler temperatures.
103
104 In the present study, we sought to investigate the effects of *SUT4*-KO on poplar seasonal growth
105 through a multi-year field trial. For comparison, we also generated single- and double-KO lines
106 of the *SUT5/SUT6* paralog (hereafter *SUT56*-KO or *sut56* for the double mutants). *SUT4*-KO but
107 not *SUT56*-KO showed accelerated leaf senescence in the fall and delayed bud flush in the
108 spring, culminating in reduced biomass growth. Moreover, *SUT4*-KO altered female catkin
109 transcriptomes in the spring which led to sterility following controlled pollination. Our data show
110 the greater importance than previously recognized of SUT4 function in tree response to
111 environmental cues of daylength and temperature.
112
113
114
115
116

Materials and Methods

Production of *sut* KO lines

The generation of the *sut4* mutants and Cas9-only vector controls in the *Populus tremula* × *alba* INRA 717-1B4 background were reported previously (Harding et al., 2022; Zhou et al., 2015). To generate the *sut5* and *sut6* single and *sut56* double mutants, gRNAs targeting individual or paralogous genes were assembled as a pair of oligos (Supplemental Table S1) into p201N-Cas9 vector behind the *Medicago truncatula U6.6* promoter, following the approach of Bewg et al. (2022). *Agrobacterium*-mediated transformation and plant regeneration was performed as described (Bewg et al., 2022).

Amplicon sequencing to determine mutation patterns

Leaves from independent events of tissue cultured plants were collected for genomic DNA extraction and amplicon sequencing library preparation (Bewg et al. 2022) using consensus primers (Supplemental Table S1). Samples were then barcoded with Illumina amplicon indexing primers, pooled, and sequenced on an Illumina MiSeq at the Georgia Genomics and Bioinformatics Core at the University of Georgia to obtain PE150 reads. Sequencing reads were processed and indel patterns identified using the Analysis of Genome Editing by Sequencing (AGEseq) program (Xue & Tsai, 2015) with a mismatch allowance set at 1%, followed by manual curation. Tetra allelic mutations were confirmed in all lines (Supplemental Table S2).

Plant propagation and field establishment

139 Multiple independent lines each for *sut4* (8), *sut5* (3), *sut6* (2), and *sut56* (3) mutants along with
140 wild-type (WT) and Cas9 controls were propagated from single-internode stem cuttings (Frost et
141 al., 2012). Cuttings were transferred to 1-gallon pots containing commercial soil mixture (Fafard
142 3B) supplemented with Osmocote (15-9-12 NPK, 3-month slow release) and placed in a walk-in
143 growth chamber for ~3 weeks (Tuma et al., 2024). Plants were moved into an adjacent
144 greenhouse for 2 weeks before transfer to a lath house within a fenced nursery at the University
145 of Georgia's Whitehall Forest for an additional 2 weeks. For logistical reasons having to do with
146 the timing of cutting establishment, *sut4* plants were slightly shorter than control plants at the
147 time of out-planting. Plants were transferred to 20-gallon pots containing a mix of Jolly Gardener
148 premium soil (75% aged pine bark, 25% peat moss) and Fafard 3B with additional Osmocote
149 (15-9-12 NPK, 3-month slow release) and planted at the nursery in summer 2021. Genotypes
150 were completely randomized throughout the site and spaced 1.5 meters apart from one another
151 (Supplemental Figure 1). The first planting occurred in early June 2021 for *sut4* mutants and
152 controls (WT and *Cas9*), and the second planting occurred in mid-August 2021 for *sut4*, *sut5*,
153 *sut6*, *sut56* and controls. Plants were watered using an overhead irrigation system. The site was
154 watered between 2-4 hours daily from early April to late October. The field trial was conducted
155 with approval from the Animal and Plant Health Inspection Service (APHIS) of the U.S.
156 Department of Agriculture.
157
158 **Field growth and phenology monitoring**
159 The diameter of the main stem ~1m above the soil surface was measured monthly or bimonthly
160 from August 2021 - April 2023. Plant height was measured from the base of the stem at soil level
161 to shoot tip in April 2022 and 2023. Trees were monitored throughout the fall to compare onset

162 and rate of leaf abscission between genotypes. Leaf color was compared between genotypes as
163 an indicator of leaf senescence on October 11th, 2022. In the spring, the appearance of bud flush
164 on the dominant stem and flowering were recorded. No floral tissues were detected in the first
165 growth season, but catkins were observed during spring of the second (late February 2023) and
166 third (early March 2024) growing seasons. The total number of trees that developed catkins was
167 recorded prior to their removal from the field site per the APHIS regulation. Further information
168 regarding the growth cycles, phenotyping, and sampling are reported in the Supplemental
169 Figures (Supplemental Figure 1).
170
171 **Tissue sampling**
172 Approximately 12 – 17 months after out planting, increment cores (10 mm in length and 2 mm in
173 diameter) were collected from the main stem ~1.3 meter above soil level using a micro-coring
174 device (Costruzioni Meccaniche Carabin C, San Vito di Cadore, Italy) according to Rossi and
175 colleagues (2006). Stems (*n* = 10-12) were approximately 2–6 cm in diameter at the time of
176 sampling. Increment cores were collected from the same stems during active growth in August
177 2022 (summer) and during dormancy in January 2023 (winter). Xylem and bark were separated
178 from the cores in the field, snap-frozen in liquid nitrogen before being transported back to
179 laboratory facilities where they were stored at -80°C until sample processing occurred.
180 Temperatures ranged from a night-time low of 22°C to a daytime high of 31°C (daily average
181 25°C) on the day of summer sampling, and from a low of 3°C to a high of 18°C (daily average
182 11°C) on the day of winter sampling (Supplemental Figure 2). Catkins were observed in
183 February 2023 after the second winter in the field. Three developmental stages of catkins were
184 collected on March 1, 2023 for metabolite and transcript profiling. All tissue sampling occurred

185 under sunny conditions between 11AM – 2PM. Tissues were snap frozen, ground under liquid
186 nitrogen with a mortar and pestle, and stored at -80°C.
187
188 **Metabolite profiling**
189 Tissues were lyophilized for 48 hours (FreezeZone 2.5, Labconco), ground through a 40-mesh
190 sieve using a Wiley Mill (Thomas Scientific), and further ball-milled to a fine powder in a S1600
191 Mini G Bead-beater (Spex SamplePrep; Metuchen, New Jersey) for metabolite profiling by Gas
192 Chromatography-Mass Spectrometry (GC-MS) as detailed previously (Harding et al., 2022;
193 Tuma et al., 2024). Peak identities were assigned based on the NIST08, FiehnLib metabolomics
194 library (Agilent) (Kind et al., 2009) and in-house spectral libraries from authentic standards (Xue
195 et al., 2013; Chen et al., 2014; Harding et al., 2022). A standard mix of succinic acid, sucrose,
196 glutamic acid, fructose, glucose, and ascorbic acid was loaded at the beginning and end of each
197 sample sequence to monitor derivatization and instrument performance. Peak intensities were
198 normalized by the internal standard and reported on a sample dry weight basis (normalized peak
199 area). Sucrose and hexose abundance (sum of fructose and glucose) was reported as µg/mg dry
200 weight.
201
202 **Starch**
203 Starch content was determined by hydrolyzing starch to glucose using enzymatic digestion with
204 α-amylase and amyloglucosidase (Chow and Landhausser, 2004) using 10 mg of lyophilized,
205 wiley- and ball-milled tissue powder as previously described (Tuma et al., 2024). Starch
206 abundance was reported as µg/mg dry weight.
207

208 **Wood chemical composition and physical property analyses**

209 Fifteen-cm long pieces of the main stem (*n* = 6) were destructively harvested following bud flush
210 in March 2023. For wood chemistry analysis, stem segments were debarked, dried at 55°C for 24
211 hours, and ground to pass through a 40-mesh screen using a Wiley mill. Samples were then run
212 through 99 cycles of hot ethanol extraction using a Soxhlet extraction unit (Buchi) and air dried.
213 Klason lignin content was determined as described (Swamy et al., 2015). The acid hydrolysates
214 were used for structural carbohydrate analysis by high-performance anion exchange according to
215 (Huntley et al., 2003). The ratio of lignin monomers in the stems (syringyl/guaiacyl, S/G ratio)
216 was determined by pyrolysis-molecular beam mass spectrometry according to Harman-Ware et
217 al. (2022). Three ~7.5 mm longitudinal wood sections were obtained from the main stem
218 approximately ~1 m above soil level for analysis of specific gravity, acoustic velocity, and
219 modulus of elasticity as described (Vieilledent et al., 2018; Tsai et al., 2020; Dahlen et al., 2023).
220

221 **RNA-seq analysis**

222 Snap-frozen catkin tissues (*n* = 3-5) were ground to a fine powder under liquid nitrogen and an
223 aliquot was used for RNA extraction using the Direct-zol RNA Miniprep kit (Zymo) with
224 PureLink Plant RNA Reagent (Life Technologies) as described (Harding et al., 2018). Illumina
225 low input RNA (with PolyA selection) library preparation and NovaSeq sequencing (NovaSeq
226 XP V1.5 reagent kits, 10B flowcell, 2 ×151 run length) were performed at the Joint Genome
227 Institute (proposal: 10.46936/10.25585/6000884). RNA-seq reads were aligned to the *Populus*
228 *tremula* haplotype of the 717 reference genome (Zhou et al., 2023) using STAR-2.7.10 (Dobin
229 and Gingeras, 2015) with the following parameters: --alignMatesGapMax 20000, --
230 alignIntronMax 10000, --outFilterScoreMinOverLread 0.1, and --outFilterMatchNminOverLread

231 0.1. Expression levels were estimated using featureCounts from the Subread package v2.0.6 with
232 the options -Q 2, -s 0, -T 12, -p, and --countReadPairs -C (Liao et al., 2014) and reported as
233 FPKM (fragments per kilobase of transcript per million mapped reads). Differential gene
234 expression analysis were performed using DESeq2 v1.34.0 (Love et al., 2014). Thresholds for
235 significant differential expression were based on minimum FPKM ≥5 in all samples of at least
236 one group, $Q \leq 0.005$, and fold change ≥1.5. Gene ontology (GO) enrichment analysis of
237 significantly up- or down-regulated genes was performed using ShinyGO v0.77 (Ge et al., 2020)
238 available at http://aspendb.uga.edu/ShinyGO/. Expression responses of selected genes were
239 visualized using the HeatMapperPlus tool (http://bar.utoronto.ca/ntools/cgi-
240 bin/ntools_heatmapper_plus.cgi).
241
242 **Controlled pollination**
243 The branches containing flower buds were collected from WT and *sut4* trees and incubated in
244 ¼MS macro salt media at room temperature in a confined laboratory to force flower. After catkin
245 flowers opened, wild *P. tremuloides* pollen sourced from Minnesota 2022 (with assistance of
246 Kathy Haiby, Poplar Innovations Inc.) was brushed onto individual WT and *sut4* catkins which
247 were then covered by glassine bags. After 7-10 days, the capsules opened, and the cottony fuss
248 was collected for observation under a dissecting microscope. The length of catkins, seed size and
249 number, and ovule size were recorded. The controlled pollination experiments were carried out
250 in both 2023 and 2024 with reproducible results.
251
252 **Statistics**

253 Repeated measures analysis of variance (ANOVA) was used to determine significant differences
254 in growth over time, genotypic effects, and their interactions using *R* v4.1.0 (R Core Team, 2016)
255 in Rstudio v.2022.12.353). All other reported genotypic contracts were assessed with Student's *t*-
256 test ($\alpha = 0.05$).
257
258
259 **Results**
260
261 *Altered phenology and reduced biomass accrual of field-grown sut4 poplar*
262 We established a field trial in summer 2021 to investigate the extent to which CRISPR-KO of
263 winter-expressed *SUT* genes would alter phenology and/or seasonal growth. Over 200 trees were
264 planted in 20-gal pots in early June (cohort 1: control and *sut4*) and mid-August (cohort 2:
265 control, *sut4*, *sut5*, *sut6*, and *sut56*). Following the first partial (2021) growth season, *sut4*
266 mutants showed signs of leaf yellowing in late October when leaves of the other genotypes
267 remained green regardless of cohort (Figure 1A). By mid-November nearly 90% of *sut4* trees
268 had lost all of their leaves while the majority of the controls and *sut5*, *sut6*, and *sut56* mutants
269 still retained the majority of their foliage (Figure 1B-C). In early December, the majority of the
270 trees had lost nearly all of their foliage (Figure 1C). Bud flush the following spring (March 2022)
271 was delayed by an average of 7 days for the *sut4* trees compared to the controls and
272 *sut5/sut6/sut56* mutants (Figure 1D). Similar trends were also observed in two subsequent years,
273 suggesting a reduced leaf lifespan in *sut4* trees.
274

Diameter of the main stems was monitored monthly for cohort 1 and bimonthly for cohort 2. For cohort 1, diameter increases during the 2022 growth season were significantly smaller in *sut4* than control trees (Figure 1E). The differential was evident by March 2022 when 88% of control trees had increased diameters versus only 31% of *sut4* trees (Figure 1F). To ascertain whether the slower spring growth was associated with slightly smaller *sut4* trees at the start of the experiment, a subset of initial size-matched 13 control and 13 *sut4* trees was examined. The same pattern was observed, with the first measurable diameter increases occurring 2-3 months later in *sut4* than in control trees (Figure 1E cohort 1 inset). Interestingly for cohort 2 that was released two months behind cohort 1, *sut4* diameter growth was reduced by a much lesser extent, whereas *sut5*, *sut6*, and *sut56* were indistinguishable from controls (Figure 1E). Closer examination confirmed a slower spring growth of *sut4* trees in cohort 2 as well. Diameter growth of *sut4* trees between February 5, 2022 (before bud break) and June 1, 2022 was half of that in control trees (Figure 1E cohort 2 inset). However, diameter growth rates were similar among genotypes through the remainder of the growth season (June to October, 2022). The 2022-2023 winter was unseasonably warm (Supplemental Figure S2) and the diameter differentials between *sut4* and the other genotypes remained constant through April 2023 before the field trial was terminated (Figure 1E). A subset of cohort 2 trees was permitted to continue, and diameter growth was monitored monthly during spring 2024. We recorded first diameter increases by April for the vast majority of control and *sut56* trees (92% for both), but only 58% of *sut4* trees (Figure 1F).

Tree height was slightly reduced, by ~10%, in *sut4* compared to the controls and *sut56* trees in April of 2022 (Figure 1G-H). At the end of the experiment, *sut4* trees were ~ 20% shorter than control and *sut56* trees (Figure 1G). Together, these results highlight altered phenology, including

298 shorter leaf lifespans and shorter cambial growth periods, as an underlying cause of the growth
299 reduction in *sut4* trees and this penalty was particularly severe for cohort 1.
300
301 *Altered NSC homeostasis in sut4 stems*
302 We compared levels of monosaccharides and oligosaccharides in the bark and xylem sampled
303 during summer and winter seasons. Because growth was unaltered in single- and double-KO of
304 *SUT5/SUT6*, only *sut56* trees were included in subsequent analyses. Sucrose was more abundant
305 in bark and xylem of *sut4* mutants than control regardless of season (Figure 2A), consistent with
306 earlier work on *SUT4*-KD and *sut4* poplars in the greenhouse (Payyavula et al., 2011; Harding et
307 al., 2022; Tuma et al., 2024). Sucrose levels changed little in *sut56* xylem or bark relative to the
308 control (Figure 2A).
309
310 Unlike sucrose, hexose (fructose and glucose) levels increased sharply between summer and
311 winter in bark and xylem of all lines (Figure 2B). Hexoses decreased in *sut4* bark in the summer
312 but increased in the winter in both bark and xylem. Hexose levels also increased in the bark of
313 *sut56* in both summer and winter (Figure 2B). As a result, the hexose-to-sucrose ratio was much
314 lower in bark of *sut4* than other lines during summer (Figure 2A-B). Bark and xylem starch
315 abundance differed little between genotypes in summer or winter and exhibited large declines of
316 similar magnitude in all genotypes during the transition to winter growth (Figure 2C).
317
318 The RFOs galactinol and raffinose and their precursor myo-inositol offer protection during cold
319 or drought (Kozlowski, 1992; ElSayed et al., 2014). Myo-inositol levels increased significantly
320 in both bark and xylem of *sut4* in summer, but not in winter when its overall abundance

321 decreased (Figure 3A). Stem galactinol and raffinose abundances were at marginally detectable
322 levels in summer but increased sharply in all genotypes during the winter (Figure 3B-C). Both
323 galactinol and raffinose levels were lower in winter *sut4* bark and xylem but changed little in
324 *sut56* relative to the controls (Figure 3B-C). The attenuated winter increases of RFOs in *sut4* are
325 consistent with a previous report of compromised induction of RFOs in drought-stressed *SUT4*-
326 KD plants (Frost et al., 2012).
327
328 *Wood physicochemical properties were altered in sut4 trees*
329 Neither lignin content nor syringyl-to-guaiacyl (S/G) monolignol ratio was altered in *sut4* or
330 *sut56* (Figure 4A-B). Acoustic velocity did not differ between genotypes (Figure 4C), However,
331 the specific gravity and the modulus of elasticity of the stem wood was reduced in both *sut4* and
332 *sut56* mutants relative to the controls (Figure 4D-E).
333
334 *Altered female catkin transcriptomes and reproductive competence in sut4*
335 Field-grown female 717 trees usually flower after 5-8 years (Mohamed et al., 2010).
336 Surprisingly, catkins were observed on many of the trees in late February through early March
337 2023 (Figure 5A) and removed immediately to comply with APHIS regulations. In total, 76% of
338 the controls and 59% of the *sut4* in cohort 1 and 30% of the controls, 45% of the *sut4*, and 22%
339 of the *sut56* in cohort 2 flowered in early March 2023 (Figure 5B). In the extended trial with a
340 subset of cohort 2 trees, 75% of the controls, 75% of the *sut4*, and 77% of the *sut56* trees
341 flowered in late February 2024 (Figure 5B). Thus, no apparent differences in flowering
342 frequency were detected between genotypes.
343

344 *SUT4* is the predominant *SUT* gene expressed in poplar flowers (Payyavula et al., 2011). To
345 assess the effects of *SUT4*-KO on catkin development, we performed GC-MS analysis on
346 unopened floral buds, newly emerged catkins, and elongating catkins (Figure 5A inset). Sucrose
347 levels remained constant during WT catkin development and changed little between genotypes in
348 dormant floral buds (Figure 5C, stage I). However, sucrose increased significantly in newly
349 emerged (stage II) and elongating catkins (stage III) of *sut4* relative to WT (Figure 5C). Hexose
350 levels increased steadily during catkin development in both genotypes and were significantly
351 higher in newly emerged catkins of *sut4* than WT (Figure 5C). Both galactinol and raffinose
352 levels were highest in the dormant buds of WT and declined to similar levels in newly emerged
353 and elongating catkins (Figure 5C). However, the RFOs remained high in *sut4* catkins. As a
354 result, galactinol levels were significantly higher in newly emerged and elongating catkins of
355 *sut4* than WT (Figure 5C). Raffinose exhibited a similar trend but was only significant in
356 elongating catkins (Figure 5C).
357
358 *Transcriptional adjustments to flavonoid biosynthesis in sut4 catkins*
359 We then performed RNA-Seq of elongating catkins and identified 821 significantly up-regulated
360 and 660 down-regulated genes in *sut4* relative to the control catkins. Gene Ontology (GO)
361 categories of 'protein oligomerization', 'cellular response to unfolded protein', 'misfolded
362 protein binding', 'protein refolding', and cellular responses to heat, hypoxia, and hydrogen
363 peroxide were over-represented among up-regulated genes (Figure 5D). Specifically, over 22%
364 of the ~380 717 genes annotated to encode various heat shock proteins (HSPs) (Yer et al., 2018)
365 were significantly up-regulated in *sut4* catkins. Also up-regulated were genes encoding several
366 heat shock factors (HSFs) and late embryogenesis abundant (LEA) proteins. Three *GolS*

367 (galactinol synthase) genes were detected in elongating catkins and all three were sharply
368 induced in *sut4* catkins, including ortholog of the *Populus alba × grandidentata Pa×gGolSII*
369 previously shown to exhibit cool season-biased expression (Unda et al., 2012). Expression of
370 raffinose synthase genes was largely unchanged. The results are consistent with significantly
371 elevated levels of galactinol, but not raffinose, in the elongating *sut4* catkins (Figure 5C).
372
373 The smaller group of down-regulated genes were enriched with GO terms associated with
374 'proanthocyanidin biosynthetic process', 'flavonoid biosynthetic process', 'response to UV-B',
375 'regulation of systemic acquired resistance', 'seed coat development', and 'mitotic cell cycle
376 phase transition' (Figure 5D). Essentially all flavonoid pathway genes and several upstream
377 regulators (Tsai et al., 2006) that were detected in catkins were significantly down-regulated in
378 *sut4* flowers (Figure 5E). All four genes encoding orthologs of *Arabidopsis* TRANSPARENT
379 TESTA12 (TT12), a multidrug and toxin extrusion (MATE)-type proton antiporter involved in
380 the vacuolar deposition of proanthocyanidin precursors (Debeaujon et al., 2001; Marinova et al.,
381 2007), were repressed in *sut4* catkins (Figure 5E). The *Arabidopsis TT12* is specifically
382 expressed in ovules and developing seed, and *tt12*, like other *tt* mutants, show impaired
383 proanthocyanidin accumulation in the seed coat (Appelhagen et al., 2014).
384
385 We next performed controlled pollination to test whether *sut4* catkins are fertile. Of the 13 WT
386 and 14 *sut4* catkins pollinated, nine of each genotype elongated and produced capsules with an
387 abundance of seed trichomes (Figure 5F). There was no significant difference in the catkin length
388 between genotypes. While WT flowers produced seed as expected, no seed was obtained from
389 any of the *sut4* capsules examined under a dissecting microscope (Figure 5G). Unfertilized

390 ovules can undergo limited development in aspens (Fechner, 1972) and they were indeed
391 observed in both WT and *sut4* samples, but they were much smaller in *sut4* than in WT (Figure
392 5G). Together with the transcriptomic changes, our results reveal a critical role of SUT4 during
393 ovule and seed development in poplar.
394
395
396 **Discussion**
397
398 Seasonal alternation between carbohydrate storage during photoautotrophic growth and
399 remobilization during heterotrophic subsistence is a hallmark of the perennial lifestyle
400 (Kozlowski, 1992; Regier et al., 2010; Tixier et al., 2019). However, disruptive effects of global
401 climate change on the timing of seasonal phenology, such as fall leaf senescence and spring bud
402 flush, are increasingly evident (Estiarte and Peñuelas, 2015; Calinger and Curtis, 2023). Here we
403 report on evidence which points toward a conditioning effect of SUT4 on the ability of poplar to
404 adapt to climate change. Our main findings were that under field conditions, CRISPR-KO of the
405 winter-biased *SUT4*, but not the other winter-expressed *SUT5/SUT6*, had detrimental effects on
406 tree growth, phenology, and reproduction.
407
408 *A role of SUT4 in seasonal phenology*
409 Several lines of evidence suggest that altered plant phenology contributed to the growth penalty
410 we observed in the *sut4* mutants. While the mechanism is not yet clear, the *sut4* trees consistently
411 exhibited premature leaf senescence, delayed spring budbreak, and delayed spring diameter
412 growth relative to control and *sut56* trees (Figure 1). This translated into a shortened growth

413 season for *sut4* trees. However, soluble sugar and starch levels were not limiting in *sut4* stems
414 during the summer and winter depletion of bark or xylem starch reserves was not impaired in
415 *sut4* mutants (Figure 2). In addition, diameter growth rates were similar between *sut4* and
416 controls during summer of 2022, 2023, and 2024 for the second cohort (Figure 1E). This is
417 consistent with previous reports of no apparent growth differences of *SUT4*-KD or KO trees
418 when compared to the control under greenhouse conditions (Payyavula et al., 2011; Frost et al.,
419 2012; Tuma et al., 2024). Nevertheless, KO effects on sucrose partitioning and sprouting
420 performance under cool temperature, short day growth conditions in coppiced stems was
421 observed (Tuma et al., 2024). Elsewhere, effects of altered carbohydrate partitioning on
422 phenology have been reported for hybrid poplar (*Populus alba* × *Populus grandidentata* Michx.)
423 by Park et al. (2009). However, growth was not negatively impacted, presumably because leaf
424 lifespan was increased following sucrose phosphate synthase overexpression in that study (Park
425 et al., 2009). These results support the idea that *sut4* effects on growth were due at least in part to
426 negative impacts of altered sucrose partitioning in stems as well as in leaves under cooler and/or
427 short-day conditions. Notably, such changes to seasonal growth were not found in the *sut5, sut6,*
428 *or sut56* trees.
429
430 Soluble sugars including RFOs act as antioxidants and osmoprotectants during periods of
431 dehydration stress such as water deficit and low temperatures (Ahmad et al., 2020). For instance,
432 raffinose and galactinol are usually detected during the dormant season or under stress conditions
433 (Regier et al., 2010; Frost et al., 2012; Richardson et al., 2013) and genes associated with their
434 biosynthesis are up-regulated in the stems of poplar and Norway spruce in the winter (Ko et al.,
435 2011; Unda et al., 2012; Jokipii-Lukkari et al., 2018). The winter increases of raffinose and

436 galactinol were smaller in the stems of *sut4* than the control and *sut56* trees (Figure 3). Thus,
437 vacuolar sucrose sequestration in *sut4* appeared to affect the accrual of RFOs associated with
438 cold tolerance and perhaps the preparation for growth resumption in the spring.
439
440 Furthermore, both sugars and RFOs serve as signaling molecules during growth, development,
441 and stress responses (Rolland et al., 2006; ElSayed et al., 2014). Sugars integrate multiple
442 environmental cues such as light, temperature, and photoperiod to modulate ROS homeostasis,
443 hormonal signaling, and circadian rhythms (Rolland et al., 2006; Román et al., 2021).
444 Specifically, accumulation of sugars has been associated with the initiation and/or acceleration of
445 leaf senescence (Wingler et al., 2005). This is consistent with hastened leaf senescence in *sut4*
446 trees with elevated sugar levels. A signaling role has also been suggested for galactinol in poplar
447 where hyper-accumulation of galactinol via overexpression of *Arabidopsis thaliana AtGolS3*
448 resulted in stunted growth and altered xylem anatomy and wood chemistry, including smaller-
449 yet-more-numerous vessels, gelatinous fibers, reduced lignin, and increased cellulose accrual
450 (Unda et al., 2017). Reduced RFO levels in the *sut4* stems could have contributed to the delay in
451 bud break and resumption of growth we observed in the spring. An alternative explanation is that
452 the nutrient recapture from senescing leaves in the *sut4* mutants was compromised and as a result
453 this delayed the spring bud flush. Together, our findings implicate a role for SUT4 in modulating
454 sugar allocation and signaling, with consequences in seasonal phenology and overall plant
455 growth.
456
457 *SUT4 modulation of proanthocyanidins and RFOs in reproductive competence*

458 High carbohydrate levels usually promote flavonoid biosynthesis, especially at low temperatures
459 (Araguirang and Richter, 2022). Given sucrose levels increased in the *sut4* catkins like many
460 other organs (Harding et al., 2022; Tuma et al., 2024), the widespread suppression of flavonoid
461 biosynthesis pathway gene expression is counterintuitive. It is possible that vacuolar sucrose
462 sequestration in *sut4* mutants led to a false "low sucrose" cue perceived by other subcellular
463 compartments. Alternatively, impaired SUT4 symport activity for vacuolar efflux of sucrose
464 might have disrupted the membrane potential and affected other proton-dependent tonoplast
465 transport systems (Martinoia, 2017). In support of this idea, we detected in *sut4* catkins down-
466 regulation of the single-copy ortholog (PtXaTreH.01G136800, Figure 5E) of *Arabidopsis TT13*
467 encoding a P-type ATPase proton pump that generates the driving force for TT12-mediated
468 proanthocyanidin delivery to the vacuole (Appelhagen et al., 2015). The coordinated down-
469 regulation of genes involved in proanthocyanidin biosynthesis and vacuolar transport machinery
470 along with widespread up-regulation of heat shock protein chaperons associated with protein
471 oligomerization, misfolding, and refolding responses provides molecular support for a potential
472 signaling role of SUT4 during catkin development.
473
474 Galactinol and raffinose are known to accumulate in dormant buds (Cox and Stushnoff, 2001;
475 Falavigna et al., 2018) as well as developing embryos and seeds to confer desiccation and/or cold
476 tolerance (Peterbauer and Richter, 2001). Their levels were highest in unopened floral buds of
477 WT poplar trees and depleted as catkins emerged and elongated. However, this developmental
478 trajectory was altered in *sut4* trees, as galactinol and raffinose levels remained high in developing
479 catkins, consistent with up-regulation of *GolS* genes in *sut4* relative to WT catkins. Elevated
480 RFOs may signify a stress status of *sut4* catkins due to altered sucrose partitioning and/or

481 impaired vacuolar proanthocyanidin deposition, or stress signaling as discussed above. The
482 overrepresentation of GO terms associated with responses to heat, hypoxia, and hydrogen
483 peroxide, and with various protein misfolding and refolding processes among genes induced in
484 *sut4* catkins is consistent with a heightened cellular stress status. Thus, multiple developmental,
485 metabolic, signaling, and stress responses were altered in developing *sut4* catkins, resulting in
486 aborted ovules and reproductive infertility.
487
488 There is precedence for impaired vacuolar SUT function that impacts plant growth. Rice (*Oryza*
489 *sativa*) mutant deficient in tonoplast *OsSUT2* showed impaired growth, reduced tiller number,
490 and reduced 1000-grain weight (Eom et al., 2011). Silencing of potato (*Solanum tuberosum*)
491 *StSUT4* affected the onset of flowering, tuberization, and circadian regulation via a proposed
492 signaling role (Chincinska et al., 2008; Chincinska et al., 2013). In *Arabidopsis*, suppression of
493 cell wall invertase genes impeded ovule development via sugar signaling not associated with
494 carbon provision (Liao et al., 2020). The present work highlights the value of field trials in
495 revealing previously underappreciated effects of SUT4 on seasonal phenology, overall biomass
496 growth, and reproduction of poplar. Amongst the winter-expressed *SUT* genes, the winter-
497 dominant *SUT4* has larger roles than *SUT5* and *SUT6* in protective metabolism during dormant
498 season for both vegetative and reproductive growth. The complex interplay between sucrose
499 partitioning, RFOs, proanthocyanidins, and phenology suggests a signaling role for SUT4 that is
500 sensitive to environmental cues.
501
502 **Conflict of interest:** None declared.
503

Funding: This work was supported in part by a National Science Foundation Graduate Research Fellowship (DGE – 1842396) to T.T.T., a Department of Energy, Office of Science, Biological and Environmental Research Program Award (DESC0023166) to C.-J.T., the Center for Bioenergy Innovation, Department of Energy, Office of Science, Biological and Environmental Research Program (Award Number ERKP886) to C-J.T and A.E.H.-W. The work (proposal: 10.46936/10.25585/6000884) conducted by the U.S. Department of Energy Joint Genome Institute https://ror.org/04xm1d337), a DOE Office of Science User Facility, is supported by the Office of Science of the U.S. Department of Energy operated under Contract No. DE-AC02-05CH11231. This work was authored in part by the Alliance for Sustainable Energy, LLC, the manager and operator of the National Renewable Energy Laboratory for the US Department of Energy (DOE) under contract no. DE-AC36-08GO28308. The views expressed in the article do not necessarily represent the views of the DOE or the US government. The US government retains and the publisher, by accepting the article for publication, acknowledges that the US government retains a nonexclusive, paid-up, irrevocable, worldwide license to publish or reproduce the published form of this work, or allow others to do so, for US government purposes.

Acknowledgements: The authors thank Gilles Pilate of INRA, France for providing poplar clone INRA 717-1B4, Batbayar Nyamdari for GC-MS assistance, Maria Ortega for guidance on pollination experiments, Hansini Fernando for assistance with sample processing, the Georgia Genomics and Bioinformatics Core at the University of Georgia (RRID:SCR_010994) for Illumina sequencing assistance, and Kathy Haiby of Poplar Innovations Inc. for aspen pollen collection.

527

528 **Authors' Contributions:** T.T.T, S.A.H, & C-J.T. conceived the study and designed all
529 experiments. T.T.T. performed all experiments and analyzed the data, with assistance from
530 H.A.M., H.P., & W.P.B. for transgenic plant production and amplicon sequencing, S.A.H for
531 metabolic analyses, B.L. for RNA extraction, A.L., K.W.B., & R.Z., for RNA-seq analysis,
532 D.L.W.W. for diameter and flower monitoring, M.D. & R.Z. for controlled pollination, J.D. for
533 wood property analysis, and S.S. & A.E.H.-W. for wood chemistry analysis. T.T.T. prepared the
534 manuscript which was revised by C.J.T. with contributions from S.A.H.

535

536 **Legends to Figures**

537

538 **FIGURE 1:** Biomass yield and growth characteristics of *sut* and control poplars.
539 (A) Representative adaxial views of leaf plastochron index (LPI)-4, LPI-6, LPI-8, LPI-10, and
540 LPI-12 prior to leaf abscission.
541 (B) Representative photos of field-grown trees taken in November 2021. Arrows denote *sut4*
542 trees.
543 (C) Progression of leaf abscission from the main stem in Fall 2021. Data represent the percentage
544 of trees per genotype that had abscised or desiccated leaves using pooled transgenic events and
545 biological replicates (n = 69 for control, n = 78 for *sut4*, n = 13 for *sut5*, n = 11 for *sut6*, and n =
546 19 for *sut56*).
547 (D) Bud flush was evaluated in the spring of 2022 based on the epicormic buds on the main
548 stem. Data represent the percentage of trees per genotype that had flushed buds using pooled

549 transgenic events and biological replicates (n = 69 for control, n = 78 for *sut4*, n = 13 for *sut5*, n

550 = 11 for *sut6*, and n = 19 for *sut56*).

551 (E) Stem diameter of trees from Cohort 1 and Cohort 2 measured 1 m above root collar monthly

552 or bi-monthly. Data are mean ± standard deviation of pooled transgenic events and biological

553 replicates (n = 40 for control or 29 for *sut4* in cohort 1, or n = 23 for control, 40 for *sut4*, 13 for

554 *sut5*, 11 for *sut6*, and 18 for *sut56* in cohort 2). The effects of time (*t),* genotype (*g),* and their

555 interaction (*t* x *g)* were assessed with a repeated measures two-way ANOVA. ***, $P \leq 0.001$.

556 Inset in cohort 1 was from size-matched control or *sut4* trees at the start of the monitoring (n =

557 13). Inset in cohort 2 represent diameter increments during spring and summer of 2022.

558 (F) Cambial growth reactivation in the spring of 2022 (cohort 1) and 2024 (cohort 2). Data

559 represent the percentage of trees per genotype that had the first measurable diameter increases,

560 with months indicated by numbers (n = 29-40 trees for cohort 1 or n = 13-24 trees for cohort 2).

561 (G) Height of dominant stem measured at the beginning of the growing season in 2022 and 2023.

562 Data are mean ± standard deviation of n = 15 – 22 trees per genotype using pooled transgenic

563 events and biological replicates. Significance was conducted using 2-sample *t*-test. *, P <0.05.

564 (H) Representative image of control, *sut4,* and *sut56* trees 14 months after field outplanting.

565

566 **FIGURE 2:** Nonstructural carbohydrate abundance in stem organs of different genotypes.

567 (A) Sucrose, (B), hexose (sum of fructose + glucose), and (C) starch abundance in bark and

568 xylem during summer and winter. Data are mean ± standard error of n = 8-12 biological

569 replicates. Significance was determined by Student's *t*-test against control. ∗, $P \leq 0.05$; ∗∗, $P \leq$

570 0.01; ∗∗∗, $P \leq 0.001$.

571

572 **FIGURE 3:** Oligosaccharide abundance dynamics in stem organs of different genotypes.

573 (A) Myo-inositol, (B), galactinol, and (C) raffinose abundance in bark and xylem during summer

574 and winter. Data are mean ± standard error of n = 8-12 biological replicates. Significance against

575 control was determined by Student's t-test. ∗, $P \leq 0.05$; ∗∗, $P \leq 0.01$; ∗∗∗, $P \leq 0.001$.

576

577 **FIGURE 4:** Wood characteristics and chemical properties.

578 (A) total lignin level, (B) syringyl-to-guaiacyl lignin (S/G) ratio, (C) acoustic velocity, (D)

579 specific gravity, and (E) modulus of elasticity. Data are mean ± standard deviation of n = 6 -12

580 biological replicates. Significance was determined against control trees by Student's t-test; ∗, $P \leq$

581 0.05; ∗∗, $P \leq 0.01$; ∗∗∗, $P \leq 0.001$.

582

583 **FIGURE 5:** Flowering phenotypes in control and *sut* trees.

584 (A) First sign of axillary inflorescence bud flushing on early spring 2023. Inset shows

585 representative catkin developmental stages used in metabolite analysis (I, unopened floral bud;

586 II, newly emerged catkin; and III, elongating catkin). Bar = 1 cm.

587 (B) Total percentage of trees per genotype from Cohort 1 and Cohort 2 that developed catkins

588 during the spring of the 2023 and 2024.

589 (C) Sucrose, hexose (sum of fructose + glucose), galactinol, and raffinose abundance in

590 unopened floral bud,s newly emerged catkins, and elongating catkins. Data are mean ± standard

591 error of n = 6-8 biological replicates. Significance was determined by Student's t-test. ∗, $P \leq$

592 0.05; ∗∗, $P \leq 0.01$; ∗∗∗, $P \leq 0.001$.

593 (D) GO enrichment of differentially up- or down-regulated genes in the elongating catkins of the
594 *sut4* mutants relative to the control. Representative GO terms with fold-enrichment >6 and gene
595 number >5 are shown.
596 (E) Significant expression response heatmaps of genes associated with flavonoid and
597 proanthocyanidin biosynthesis and regulation. Log_2FC, log_2-transformed fold-change
598 (*sut4*/control) of $n = 7$ (pooled from 5 WT and 3 *Cas9*) and 5 (*sut4*) biological replicates. ANR,
599 anthocyanidin reductase; ANS, anthocyanidin synthase; CHS, chalcone synthases; CHI, chalcone
600 isomerase; DFR, dihydroflavonol reductase; F3H, flavanone 3-hydroxylase; F3'H, flavonoid
601 3′-hydroxylase; F3'5'H, flavonoid 3′,5′-hydroxylase; LAR, leucoanthocyanidin reductase; TT,
602 transparent testa.
603 (F) Representative *sut4* capsules with seed trichomes after controlled pollination.
604 (G) Visual representation of seeds and ovules from control and *sut4* catkins. Scale bar = 1 mm.
605
606
607 **References**

608 **Ahmad F, Singh A, Kamal A** (2020) Osmoprotective role of sugar in mitigating abiotic stress
609 in plants. *In* Protective chemical agents in the amelioration of plant abiotic stress, pp 53-
610 70
611 **Ameglio T, Decourteix M, Alves G, Valentin V, Sakr S, Julien JL, Petel G, Guilliot A,**
612 **Lacointe A** (2004) Temperature effects on xylem sap osmolarity in walnut trees:
613 evidence for a vitalistic model of winter embolism repair. Tree Physiology **24:** 785-793
614 **Appelhagen I, Nordholt N, Seidel T, Spelt K, Koes R, Quattrochio F, Sagasser M,**
615 **Weisshaar B** (2015) TRANSPARENT TESTA 13 is a tonoplast P3A-ATPase required
616 for vacuolar deposition of proanthocyanidins in Arabidopsis thaliana seeds. The Plant
617 Journal **82:** 840-849
618 **Appelhagen I, Thiedig K, Nordholt N, Schmidt N, Huep G, Sagasser M, Weisshaar B**
619 (2014) Update on transparent testa mutants from Arabidopsis thaliana: characterisation of
620 new alleles from an isogenic collection. Planta **240:** 955-970
621 **Araguirang GE, Richter AS** (2022) Activation of anthocyanin biosynthesis in high light – what
622 is the initial signal? New Phytologist **236:** 2037-2043

Calinger K, Curtis P (2023) A century of climate warming results in growing season extension: Delayed autumn leaf phenology in north central North America. PLOS ONE **18:** e0282635

Chen H-Y, Babst BA, Nyamdari B, Hu H, Sykes R, Davis MF, Harding SA, Tsai C-J (2014) Ectopic expression of a loblolly pine Class II 4-coumarate:CoA ligase alters soluble phenylpropanoid metabolism but not lignin biosynthesis in Populus. Plane Cell Physiology **55:** 1669-1678

Chincinska I, Gier K, Krügel U, Liesche J, He H, Grimm B, Harren F, Cristescu S, Kuehn C (2013) Photoperiodic regulation of the sucrose transporter StSUT4 affects the expression of circadian-regulated genes and ethylene production. Frontiers in Plant Science **4**

Chincinska IA, Liesche J, Krugel U, Michalska J, Geigenberger P, Grimm B, Kühn C (2008) Sucrose transporter StSUT4 from potato affects flowering, tuberization, and shade avoidance response. Plant Physiology **146:** 515-528

Chow PS, Landhausser SM (2004) A method for routine measurements of total sugar and starch content in woody plant tissues. Tree Physiology **24:** 1129-1136

Cooke JEK, Eriksson ME, Junttila O (2012) The dynamic nature of bud dormancy in trees: environmental control and molecular mechanisms. Plant, Cell & Environment **35:** 1707-1728

Cox SE, Stushnoff C (2001) Temperature-related shifts in soluble carbohydrate content during dormancy and cold acclimation in Populus tremuloides. Canadian Journal of Forest Research **31:** 730-737

Dahlen J, Auty D, Eberhardt TL, Schimleck L, Pokhrel NR (2023) Determination of ring-level dynamic modulus of elasticity in loblolly pine from measurements of ultrasonic velocity and specific gravity. Forestry: An International Journal of Forest Research **96:** 588-604

Debeaujon I, Peeters AJM, Léon-Kloosterziel KM, Koornneef M (2001) The TRANSPARENT TESTA12 gene of Arabidopsis encodes a multidrug secondary transporter-like protein required for flavonoid sequestration in vacuoles of the seed coat endothelium. The Plant Cell **13:** 853-871

Dobbelstein E, Fink D, Öner-Sieben S, Czempik L, Lohaus G (2018) Seasonal changes of sucrose transporter expression and sugar partitioning in common European tree species. Tree Physiology **39:** 284-299

Dobin A, Gingeras TR (2015) Mapping RNA-seq reads with STAR. Curr Protoc Bioinformatics **51:** 11.14.11-11.14.19

ElSayed AI, Rafudeen MS, Golldack D (2014) Physiological aspects of raffinose family oligosaccharides in plants: protection against abiotic stress. Plant Biology **16:** 1-8

Eom JS, Cho JI, Reinders A, Lee SW, Yoo Y, Tuan PQ, Choi SB, Bang G, Park YI, Cho MH, Bhoo SH, An G, Hahn TR, Ward JM, Jeon JS (2011) Impaired function of the tonoplast-localized sucrose transporter in rice, OsSUT2, limits the transport of vacuolar reserve sucrose and affects plant growth. Plant Physiology **157:** 109-119

Estiarte M, Peñuelas J (2015) Alteration of the phenology of leaf senescence and fall in winter deciduous species by climate change: effects on nutrient proficiency. Glob Chang Biol **21:** 1005-1017

Falavigna VdS, Porto DD, Miotto YE, Santos HPd, Oliveira PRDd, Margis-Pinheiro M, Pasquali G, Revers LF (2018) Evolutionary diversification of galactinol synthases in

669 Rosaceae: adaptive roles of galactinol and raffinose during apple bud dormancy. Journal
670 of Experimental Botany **69:** 1247-1259
671 **Fechner GH** (1972) Development of the pistillate flower of Populus tremuloides following
672 controlled pollination. Canadian Journal of Botany **50:** 2503-2509
673 **Frost CJ, Nyamdari B, Tsai C-J, Harding SA** (2012) The tonoplast-localized sucrose
674 transporter in Populus (PtaSUT4) regulates whole-plant water relations, responses to
675 water stress, and photosynthesis. PLoS ONE **7:** e44467
676 **Furze ME, Huggett BA, Aubrecht DM, Stolz CD, Carbone MS, Richardson AD** (2019)
677 Whole-tree nonstructural carbohydrate storage and seasonal dynamics in five temperate
678 species. New Phytologist **221:** 1466-1477
679 **Ge SX, Jung D, Yao R** (2020) ShinyGO: a graphical gene-set enrichment tool for animals and
680 plants. Bioinformatics **36:** 2628-2629
681 **Harding SA, Frost CJ, Tsai C-J** (2020) Defoliation-induced compensatory transpiration is
682 compromised in *SUT4*-RNAi *Populus*. Plant Direct **4:** e00268
683 **Harding SA, Hu H, Nyamdari B, Xue L-J, Naran R, Tsai C-J** (2018) Tubulins, rhythms and
684 cell walls in poplar leaves: it's all in the timing. Tree Physiology **38:** 397-408
685 **Harding SA, Tuma TT, Aulakh K, Ortega MA, Ci D, Ou Y, Tsai C-J** (2022) Tonoplast
686 sucrose trafficking modulates starch utilization and water deficit behavior in poplar
687 leaves. Plant and Cell Physiology **63:** 1117-1129
688 **Harman-Ware AE, Happs RM, Macaya-Sanz D, Doeppke C, Muchero W, DiFazio SP**
689 (2022) Abundance of Major Cell Wall Components in Natural Variants and Pedigrees of
690 Populus trichocarpa. Front Plant Sci **13:** 757810
691 **Huntley SK, Ellis D, Gilbert M, Chapple C, Mansfield SD** (2003) Significant increases in
692 pulping efficiency in C4H-F5H-transformed poplars: improved chemical savings and
693 reduced environmental toxins. Journal of Agricultural and Food Chemistry **51:** 6178-
694 6183
695 **Jokipii-Lukkari S, Delhomme N, Schiffthaler B, Mannapperuma C, Prestele J, Nilsson O,**
696 **Street NR, Tuominen H** (2018) Transcriptional roadmap to seasonal variation in wood
697 formation of norway spruce. Plant Physiology **176:** 2851-2870
698 **Keunen ELS, Peshev D, Vangronsveld J, Van Den Ende WIM, Cuypers ANN** (2013) Plant
699 sugars are crucial players in the oxidative challenge during abiotic stress: extending the
700 traditional concept. Plant, Cell & Environment **36:** 1242-1255
701 **Kind T, Wohlgemuth G, Lee DY, Lu Y, Palazoglu M, Shahbaz S, Fiehn O** (2009) FiehnLib:
702 mass spectral and retention index libraries for metabolomics based on quadrupole and
703 time-of-flight gas chromatography/mass spectrometry. Anal Chem **81:** 10038-10048
704 **Ko J-H, Prassinos C, Keathley D, Han K-H, Li C** (2011) Novel aspects of transcriptional
705 regulation in the winter survival and maintenance mechanism of poplar. Tree Physiology
706 **31:** 208-225
707 **Kozlowski TT** (1992) Carbohydrate sources and sinks in woody plants. The Botanical Review
708 **58:** 107-222
709 **Kuster TM, Dobbertin M, Günthardt-Goerg MS, Schaub M, Arend M** (2014) A
710 phenological timetable of oak growth under experimental drought and air warming.
711 PLOS ONE **9:** e89724
712 **Liao S, Wang L, Li J, Ruan Y-L** (2020) Cell wall invertase is essential for ovule development
713 through sugar signaling rather than provision of carbon nutrients. Plant Physiology **183:**
714 1126-1144

715 **Liao Y, Smyth GK, Shi W** (2014) featureCounts: an efficient general purpose program for
716 assigning sequence reads to genomic features. Bioinformatics **30:** 923-930
717 **Loescher WH, McCamant T, Keller JD** (1990) Carbohydrate reserves, translocation, and
718 storage in woody plant roots. HortScience HortSci **25:** 274-281
719 **Love M, Huber W, Anders S** (2014) Moderated estimation of fold change and dispersion for
720 RNA-seq data with DESeq2. Genome Biology **15:** 550
721 **Mahboubi A, Ratke C, Gorzsás A, Kumar M, Mellerowicz EJ, Niittylä T** (2013) Aspen
722 SUCROSE TRANSPORTER3 allocates carbon into wood fibers. Plant Physiology **163:**
723 1729-1740
724 **Marinova K, Pourcel L, Weder B, Schwarz M, Barron D, Routaboul J-M, Debeaujon I,**
725 **Klein M** (2007) The Arabidopsis MATE Transporter TT12 Acts as a Vacuolar
726 Flavonoid/H+-Antiporter Active in Proanthocyanidin-Accumulating Cells of the Seed
727 Coat. The Plant Cell **19:** 2023-2038
728 **Martínez-Vilalta J, Sala A, Asensio D, Galiano L, Hoch G, Palacio S, Piper FI, Lloret F**
729 (2016) Dynamics of non-structural carbohydrates in terrestrial plants: a global synthesis.
730 Ecological Monographs **86:** 495-516
731 **Martinoia E** (2017) Vacuolar Transporters – Companions on a Longtime Journey. Plant
732 Physiology **176:** 1384-1407
733 **Mohamed R, Wang C-T, Ma C, Shevchenko O, Dye SJ, Puzey JR, Etherington E, Sheng X,**
734 **Meilan R, Strauss SH, Brunner AM** (2010) *Populus CEN/TFL1* regulates first onset of
735 flowering, axillary meristem identity and dormancy release in *Populus*. Plant Journal **62:**
736 674-688
737 **Palacio S, Camarero JJ, Maestro M, Alla AQ, Lahoz E, Montserrat-Martí G** (2018) Are
738 storage and tree growth related? Seasonal nutrient and carbohydrate dynamics in
739 evergreen and deciduous Mediterranean oaks. Trees **32:** 777-790
740 **Park J-Y, Canam T, Kang K-Y, Unda F, Mansfield SD** (2009) Sucrose phosphate synthase
741 expression influences poplar phenology. Tree Physiology **29:** 937-946
742 **Payyavula RS, Tay KHC, Tsai C-J, Harding SA** (2011) The sucrose transporter family in
743 Populus: The importance of a tonoplast PtaSUT4 to biomass and carbon partitioning.
744 Plant Journal **65:** 757-770
745 **Peng D, Xue L-J, Gu X, Leebens-Mack JH, Tsai C-J** (2014) Bayesian phylogeny of sucrose
746 transporters: Ancient origins, differential expansion and convergent evolution in
747 monocots and dicots. Frontiers in Plant Science **5:** 615
748 **Peterbauer T, Richter A** (2001) Biochemistry and physiology of raffinose family
749 oligosaccharides and galactosyl cyclitols in seeds. Seed Science Research **11:** 185-197
750 **Regier N, Streb S, Zeeman SC, Frey B** (2010) Seasonal changes in starch and sugar content of
751 poplar (Populus deltoides × nigra cv. Dorskamp) and the impact of stem girdling on
752 carbohydrate allocation to roots. Tree Physiology **30:** 979-987
753 **Richardson AD, Carbone MS, Keenan TF, Czimczik CI, Hollinger DY, Murakami P,**
754 **Schaberg PG, Xu X** (2013) Seasonal dynamics and age of stemwood nonstructural
755 carbohydrates in temperate forest trees. New Phytologist **197:** 850-861
756 **Rohde A, Bhalerao RP** (2007) Plant dormancy in the perennial context. Trends in Plant Science
757 **12:** 217-223
758 **Rolland F, Baena-Gonzalez E, Sheen J** (2006) Sugar sensing and signaling in plants:
759 Conserved and novel mechanisms. Annual Review of Plant Biology **57:** 675-709

760 **Román Á, Li X, Deng D, Davey JW, James S, Graham IA, Haydon MJ** (2021) Superoxide is
761 promoted by sucrose and affects amplitude of circadian rhythms in the evening.
762 Proceedings of the National Academy of Sciences **118:** e2020646118
763 **Savage JA, Chuine I** (2021) Coordination of spring vascular and organ phenology in deciduous
764 angiosperms growing in seasonally cold climates. New Phytologist **230:** 1700-1715
765 **Schrader J, Moyle R, Bhalerao R, Hertzberg M, Lundeberg J, Nilsson P, Bhalerao RP**
766 (2004) Cambial meristem dormancy in trees involves extensive remodelling of the
767 transcriptome. Plant Journal **40:** 173-187
768 **Sreedasyam A, Plott C, Hossain MS, Lovell John T, Grimwood J, Jenkins Jerry W, Daum**
769 **C, Barry K, Carlson J, Shu S, Phillips J, Amirebrahimi M, Zane M, Wang M,**
770 **Goodstein D, Haas Fabian B, Hiss M, Perroud P-F, Jawdy Sara S, Yang Y, Hu R,**
771 **Johnson J, Kropat J, Gallaher Sean D, Lipzen A, Shakirov Eugene V, Weng X,**
772 **Torres-Jerez I, Weers B, Conde D, Pappas Marilia R, Liu L, Muchlinski A, Jiang H,**
773 **Shyu C, Huang P, Sebastian J, Laiben C, Medlin A, Carey S, Carrell Alyssa A,**
774 **Chen J-G, Perales M, Swaminathan K, Allona I, Grattapaglia D, Cooper**
775 **Elizabeth A, Tholl D, Vogel John P, Weston DJ, Yang X, Brutnell Thomas P,**
776 **Kellogg Elizabeth A, Baxter I, Udvardi M, Tang Y, Mockler Todd C, Juenger**
777 **Thomas E, Mullet J, Rensing Stefan A, Tuskan Gerald A, Merchant Sabeeha S,**
778 **Stacey G, Schmutz J** (2023) JGI Plant Gene Atlas: an updateable transcriptome resource
779 to improve functional gene descriptions across the plant kingdom. Nucleic Acids
780 Research **51:** 8383-8401
781 **Swamy PS, Hu H, Pattathil S, Maloney VJ, Xiao H, Xue L-J, Chung J-D, Johnson VE, Zhu**
782 **Y, Peter GF, Hahn MG, Mansfield SD, Harding SA, Tsai C-J** (2015) Tubulin
783 perturbation leads to unexpected cell wall modifications and affects stomatal behaviour in
784 Populus. Journal of Experimental Botany **66:** 6507-6518
785 **Tixier A, Gambetta GA, Godfrey J, Orozco J, Zwieniecki MA** (2019) Non-structural
786 carbohydrates in dormant woody perennials; the tale of winter survival and spring arrival.
787 Frontiers in Forests and Global Change **2**
788 **Tsai C-J, Harding SA, Tschaplinski TJ, Lindroth RL, Yuan Y** (2006) Genome-wide analysis
789 of the structural genes regulating defense phenylpropanoid metabolism in Populus. New
790 Phytologist **172:** 47-62
791 **Tsai C-J, Xu P, Xue L-J, Hu H, Nyamdari B, Naran R, Zhou X, Goeminne G, Gao R,**
792 **Gjersing E, Dahlen J, Pattathil S, Hahn MG, Davis M, Ralph J, Boerjan WA,**
793 **Harding SA** (2020) Compensatory guaiacyl lignin biosynthesis at the expense of
794 syringyl lignin in *4CL1*-knockout poplar. Plant Physiology **183:** 123-136
795 **Tuma TT, Nyamdari B, Hsieh C, Chen Y-H, Harding SA, Tsai C-J** (2024) Perturbation of
796 tonoplast sucrose transport alters carbohydrate utilization for seasonal growth and
797 defense metabolism in coppiced poplar. Tree Physiology **44**
798 **Unda F, Canam T, Preston L, Mansfield SD** (2012) Isolation and characterization of galactinol
799 synthases from hybrid poplar. J Exp Bot **63:** 2059-2069
800 **Unda F, Kim H, Hefer C, Ralph J, Mansfield SD** (2017) Altering carbon allocation in hybrid
801 poplar (Populus alba × grandidentata) impacts cell wall growth and development. Plant
802 Biotechnology Journal **15:** 865-878
803 **Vieilledent G, Fischer FJ, Chave J, Guibal D, Langbour P, Gérard J** (2018) New formula
804 and conversion factor to compute basic wood density of tree species using a global wood
805 technology database. American Journal of Botany **105:** 1653-1661

806 **Wingler A, Purdy S, MacLean JA, Pourtau N** (2005) The role of sugars in integrating
807 environmental signals during the regulation of leaf senescence. Journal of Experimental
808 Botany **57:** 391-399
809 **Xue L-J, Frost CJ, Tsai C-J, Harding SA** (2016) Drought response transcriptomics are altered
810 in poplar with reduced tonoplast sucrose transporter expression. Scientific Reports **6:**
811 33655
812 **Xue L-J, Guo W, Yuan Y, Anino EO, Nyamdari B, Wilson MC, Frost CJ, Chen H-Y, Babst**
813 **BA, Harding SA, Tsai C-J** (2013) Constitutively elevated salicylic acid levels alter
814 photosynthesis and oxidative state, but not growth in transgenic Populus. Plant Cell **25:**
815 2714-2730
816 **Yer EN, Baloglu MC, Ayan S** (2018) Identification and expression profiling of all Hsp family
817 member genes under salinity stress in different poplar clones. Gene **678:** 324-336
818 **Zhou R, Jenkins JW, Zeng Y, Shu S, Jang H, Harding SA, Williams M, Plott C, Barry**
819 **KW, Koriabine M, Amirebrahimi M, Talag J, Rajasekar S, Grimwood J, Schmitz**
820 **RJ, Dawe RK, Schmutz J, Tsai C-J** (2023) Haplotype-resolved genome assembly of
821 *Populus tremula* × *P. alba* reveals aspen-specific megabase satellite DNA. Plant Journal
822 **16:** 1003-1017
823 **Zohner CM, Renner SS, Sebald V, Crowther TW** (2021) How changes in spring and autumn
824 phenology translate into growth-experimental evidence of asymmetric effects. Journal of
825 Ecology **109:** 2717-2728
826

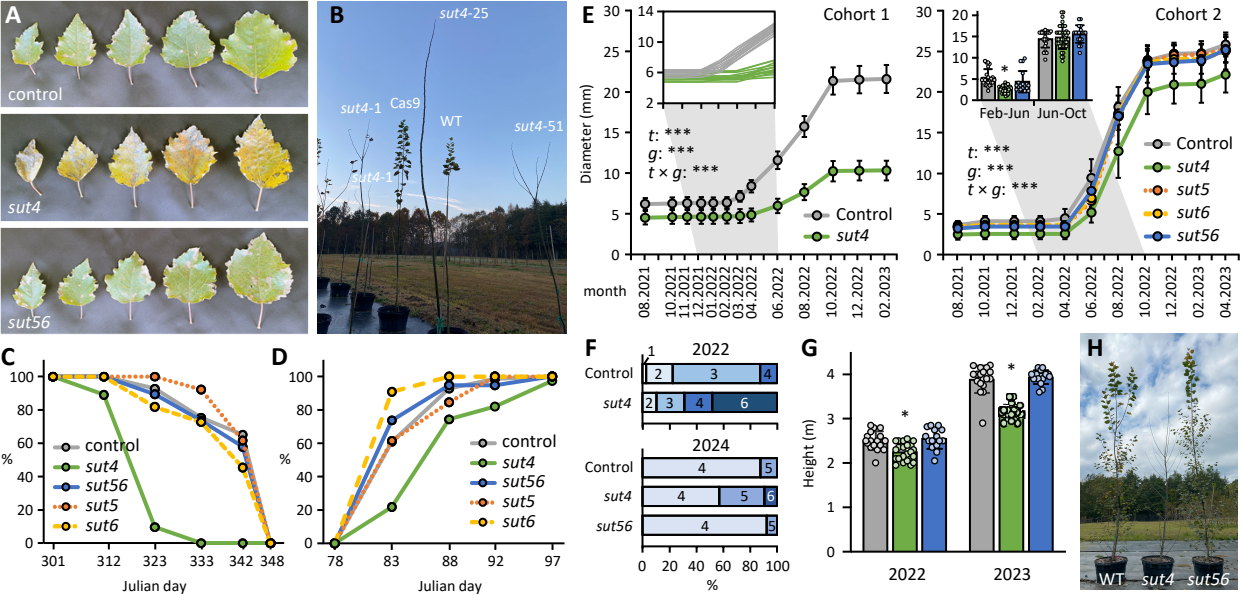
A
control
sut4
sut56
B
sut4-25
sut4-1
Cas9
WT
sut4-51
sut4-1
C
control
sut4
sut56
sut5
sut6
%
Julian day
D
control
sut4
sut56
sut5
sut6
%
Julian day
E
Cohort 1
Cohort 2
Diameter (mm)
t: ***
g: ***
t × g: ***
Control
sut4
sut5
sut6
sut56
Feb-Jun
Jun-Oct
month
F
2022
2024
Control
sut4
sut56
%
G
Height (m)
2022
2023
H
WT
sut4
sut56

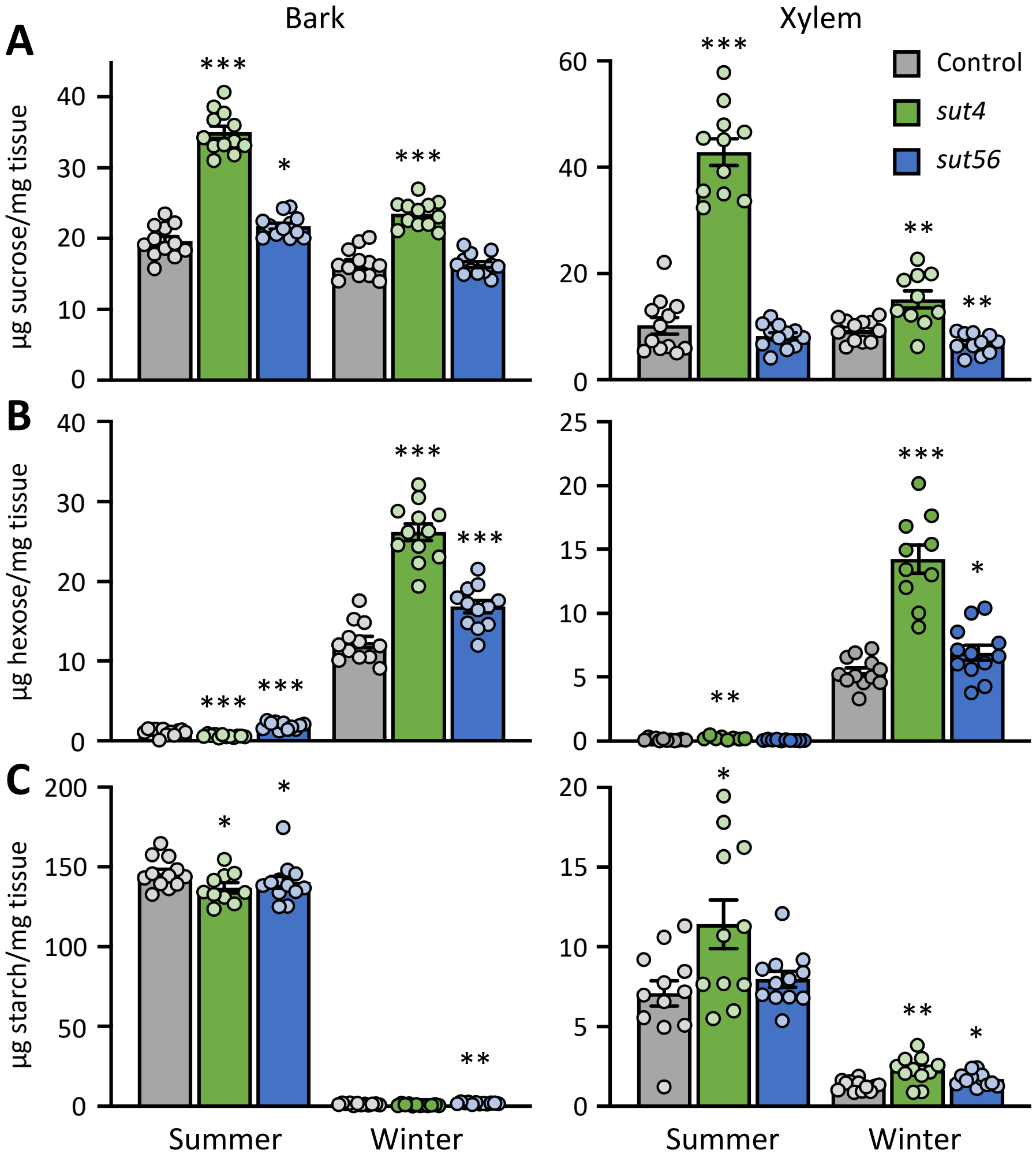
Bark
Xylem
A
B
C
Control
sut4
sut56
µg sucrose/mg tissue
µg hexose/mg tissue
µg starch/mg tissue
Summer
Winter
Summer
Winter

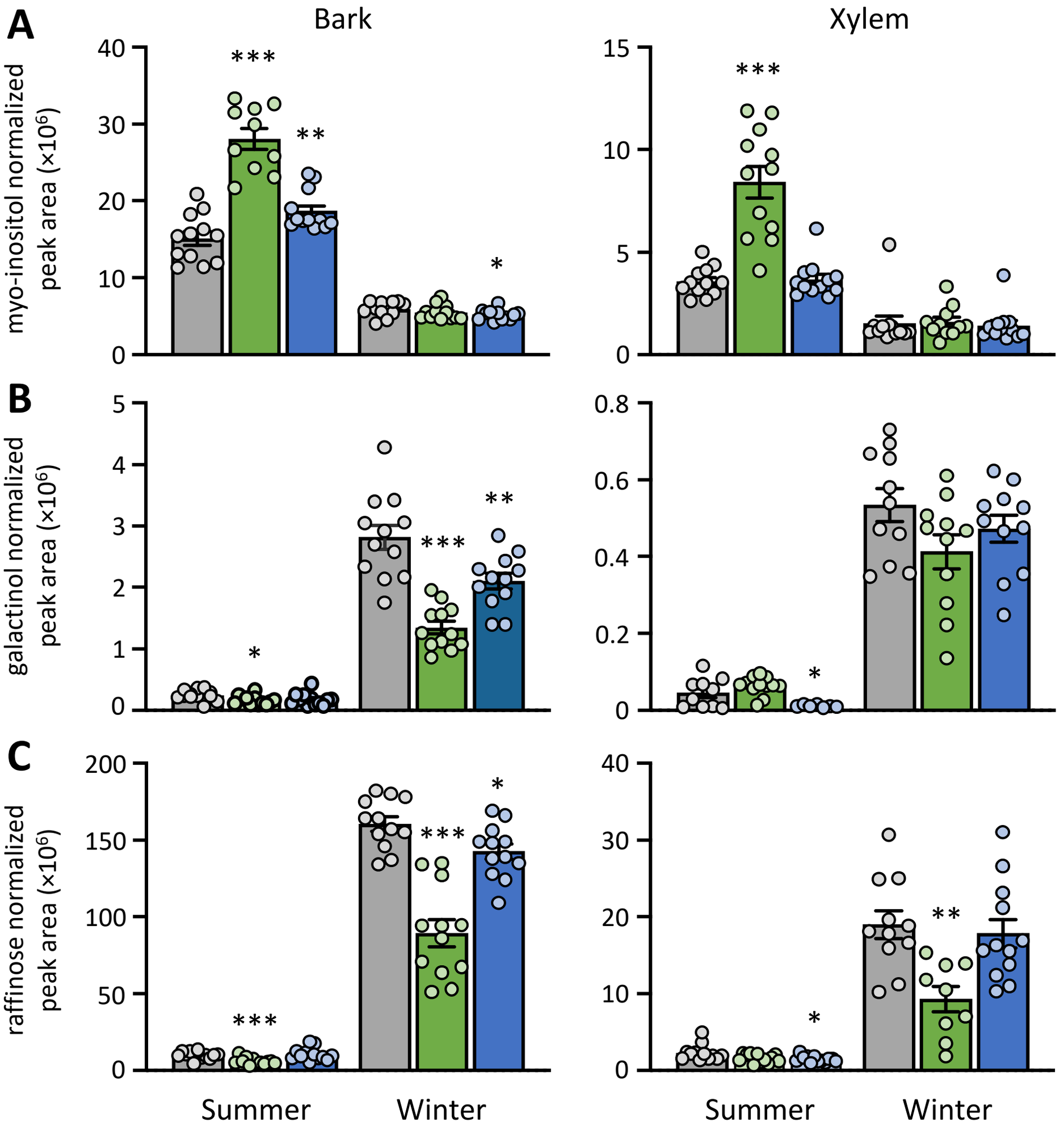
A
Bark
Xylem
myo-inositol normalized peak area (×10^6)
40
30
20
10
0
15
10
5
0
***
**
*
***
B
galactinol normalized peak area (×10^6)
5
4
3
2
1
0
0.8
0.6
0.4
0.2
0
*
***
**
*
C
raffinose normalized peak area (×10^6)
200
150
100
50
0
40
30
20
10
0
***
***
*
*
**
Summer
Winter
Summer
Winter

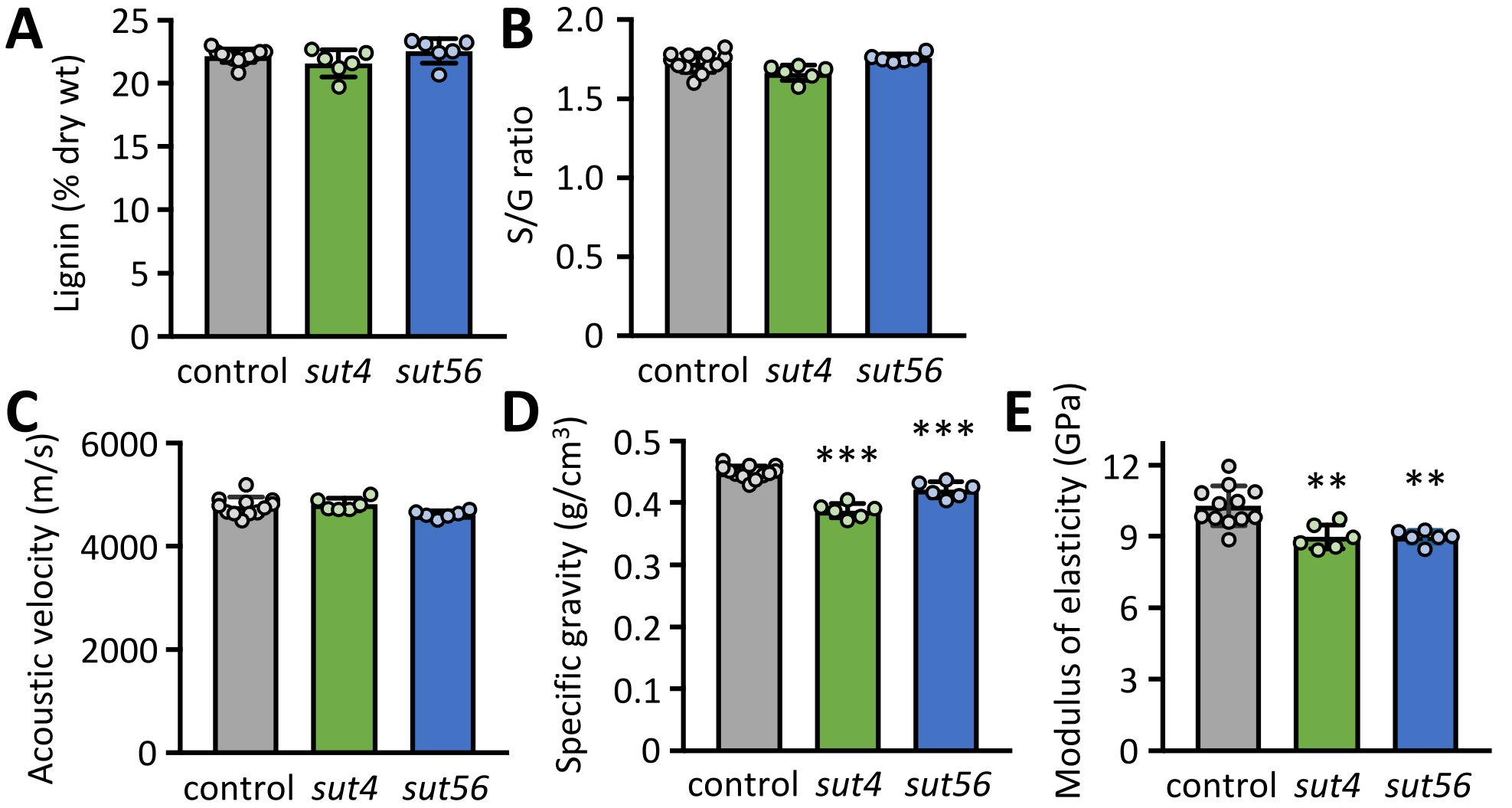
A
Lignin (% dry wt)
25
20
15
10
5
0
control
sut4
sut56
B
S/G ratio
2.0
1.5
1.0
0.5
0
control
sut4
sut56
C
Acoustic velocity (m/s)
6000
4000
2000
0
control
sut4
sut56
D
Specific gravity (g/cm3)
0.5
0.4
0.3
0.2
0.1
0
***
***
control
sut4
sut56
E
Modulus of elasticity (GPa)
12
9
6
3
0
**
**
control
sut4
sut56

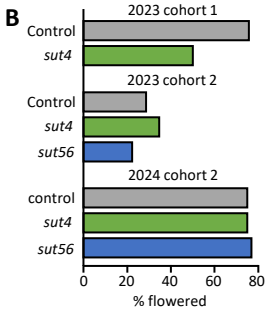

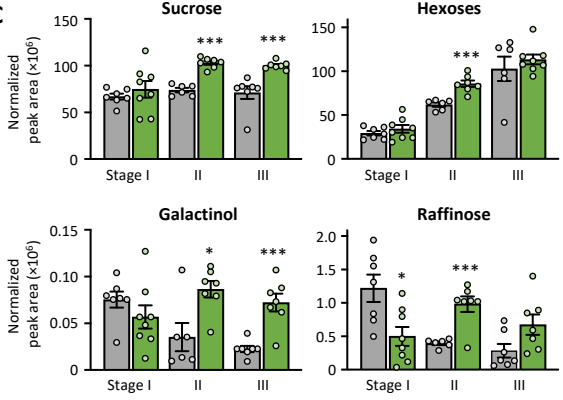

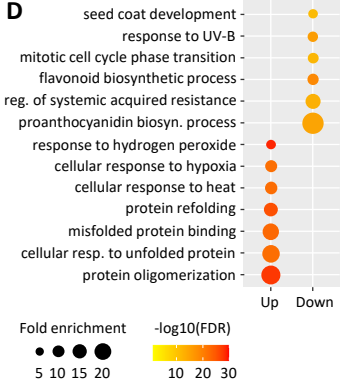

E

Gene model	Log_2FC	name
PtXaTreH.14G116200	-0.9	CHS
PtXaTreH.01G043200	-1.7	CHS
PtXaTreH.01G043300	-1.6	CHS
PtXaTreH.10G178000	-1	CHI
PtXaTreH.05G089200	-1.3	F3H
PtXaTreH.05G089100	-1.3	F3H
PtXaTreH.13G063700	-0.7	F3'H
PtXaTreH.09G055400	-1.6	F3'5'H
PtXaTreH.02G029100	-1.4	DFR
PtXaTreH.05G177900	-1.1	DFR
PtXaTreH.03G097500	-1.6	ANS
PtXaTreH.01G094900	-1.2	ANS
PtXaTreH.04G021600	-1.4	ANR
PtXaTreH.08G095200	-1.1	LAR
PtXaTreH.10G109000	-1.3	LAR
PtXaTreH.15G039500	-1.8	LAR
PtXaTreH.06G183200	-0.7	TT2
PtXaTreH.02G046300	-0.9	TT8
PtXaTreH.05G157900	-1.7	TT12
PtXaTreH.05G157600	-1.6	TT12
PtXaTreH.02G047100	-1.5	TT12
PtXaTreH.01G136800	-0.8	TT13

-0.2 … -2